Hindawi
Modelling and Simulation in Engineering
Volume 2019, Article ID 7468478, 9 pages
https://doi.org/10.1155/2019/7468478

Research Article

Optimal Stroke Path for Reciprocating Heat Engines

Mahmoud Huleihil

The Arab Academic Institute of Education, Beit-Berl College, Kfar Saba 44905, Israel

Correspondence should be addressed to Mahmoud Huleihil; mahmud.ana@gmail.com

Received 3 August 2018; Revised 30 October 2018; Accepted 21 November 2018; Published 2 January 2019

Academic Editor: Farouk Yalaoui

By testing piston motion in reciprocating heat engines as a control variable, one could find piston trajectories, different from the conventional near sinusoidal motion that should increase power production. This results from minimizing frictional losses. The purpose of this study is to determine piston trajectories that are optimal for noncombustion strokes in reciprocating engines, in the sense of minimizing frictional dissipation and hence maximizing efficiency and power. The optimal piston traces for noncombustion strokes are determined by using a combination of optimal control theory and models for the thermodynamic irreversibilities. Hence, the results are germane to external combustion engines and to the noncombustion strokes of internal combustion engines. The optimal piston traces or trajectories obtained here can be viewed as some of the building blocks from which optimal overall cycles can be constructed.

1. Introduction

Internal combustion engines [1–3] are studied using the methods of finite-time thermodynamics [4, 5]. Two modeling approaches are pursued to optimize heat engines for maximum power production: optimization for a given trajectory or thermodynamic cycle [6–16] and optimization seeking optimal trajectory by applying the methods of optimal control theory (Pontryagin's maximum principle) [17, 18, 19].

One possible way to increase the power delivery of reciprocating heat engines is to vary the piston trajectory relative to its conventional near sinusoidal motion [17]. The idea of treating piston motion as a control variable in an attempt to minimize thermodynamic losses and hence maximize power production was raised in [17, 18], in which attempts were made to find the optimal piston trajectory for Otto and Diesel cycle engines. The exercise was performed by using optimal control theory in concerts with models for the key thermodynamic irreversibilities [17, 18]. An important finding in these works was that the potential improvement in the efficiency of the reciprocating engines is not negligible and could be as high as 10–15% of current engine efficiencies. The improvements stem from lowering frictional dissipation, and heat leaks in the internal combustion engine cycles considered.

These earlier analyses, however, adopted oversimplified models for the influence of combustion processes on engine dynamics [20, 21]. Two other limitations were that (1) the heat generated due to friction was modeled as being totally transferred to the engine cooling system, namely, none of that resulted in the heating of the engine working fluid and (2) the only type of friction considered was the rubbing friction of a piston well-lubricated cylinder surface, where power dissipation goes as the square of piston speed.

The aim of this study is to determine piston trajectories that are optimal for noncombustion strokes in reciprocating engines, in the sense of minimizing frictional dissipation and hence maximizing efficiency and power. In this study, we determine the optimal piston trajectories for the strokes of reciprocating heat engines, in the sense of maximizing power production. However, we restrict our analyses to noncombustion strokes due to the complex nature of modeling combustion and its influence on engine performance. The complex models dictate pure numerical solutions. Among the benefits of doing this is the capability of the analytical solution to enable more explicit and transparent results. Hence, our results are directly applicable to external combustion engines and to the noncombustion strokes of internal combustion engines.

Although we restrict the study to noncombustion strokes, the same methods of optimal control theory could be used to optimize combustion strokes as was done in [17, 18, 19].

The two key irreversibilities modeled are friction and heat leak, and a range of friction sources are considered: mechanical and/or fluid friction. In addition, our results account for frictional dissipation heating the engine working fluid.

The piston trajectories we determine could hence be viewed as some of the building blocks from which one can calculate the optimal piston motion for various engine cycles. In addition, one would have to calculate the fraction of the total cycle time allotted to each stroke to tailor the results to the particulars of any engine cycle under consideration. These are the cycle-specific calculations.

The achievable maximum power with these optimal piston trajectories will be compared to the power that can be attained with conventional near sinusoidal piston motion. Furthermore, sensitivity studies on important engine parameters such as compression ratio, maximum piston acceleration, type of friction (i.e., functional dependence on piston speed), and the degree to which frictional dissipation heats up the engine working fluid are performed. The potential improvements in engine power for the strokes analyzed here shown to be of the order of few percent.

2. Formulation of the Problem and Modeling Assumptions

Figure 1 is a schematic of the system analyzed here: a piston moving inside a cylinder of fixed, given cross-sectional area A. The piston moves along the vertical axis, and the volume V of the working fluid can change from a maximum value of $V_{\max}$ to a minimum value of $V_{\min}$, with the engine compression ratio r defined as $r = V_{\max}/V_{\min}$. Piston motion as a function of time during the stroke is described by the time evolution of the gas volume $V(t)$, or, equivalently, piston position $x(t) = V(t)/A$. Piston velocity is described by $\dot{x}(t) = dx(t)/dt$. For the convenience of analysis in what follows, piston velocity is defined as positive for a given stroke. The steady-state operation is only analyzed: namely, start-up and turnoff transients are not considered.

The general picture could also include a regenerator inside the cylinder, as well as two-piston cylinders, as illustrated in Figure 2. Stirling and related cycles are pertinent examples. In that case, we adopt the approximation suitable for current high-quality regenerators of a regeneration effectiveness of close to 100%. Namely, the ratio of the heat exchanged in the regenerator to the heat stored in the regenerator is essentially unity [22–24]. However, as the gas passes through the regenerator, fluid friction losses will occur and are accounted for in our model.

The ideal-gas approximation is adequate for most engine operating conditions and permits closed analytical solutions to be derived. The formalism described below can also be used for real gas behavior, but results would then have to be generated numerically [17, 18, 20–24].

The types of noncombustion engine strokes included in our analysis are compression, expansion, and constant volume. The two former types of strokes are found in all engine cycles, and the latter is relevant for Stirling cycles, among others.

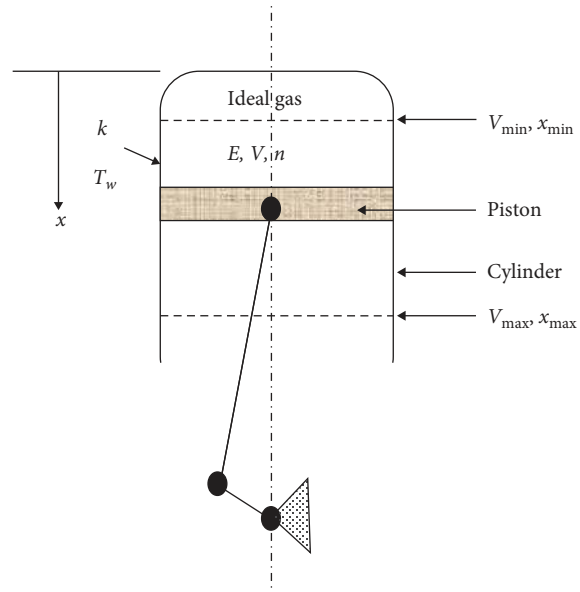

Figure 1: Schematic of the reciprocating engine cylinder.

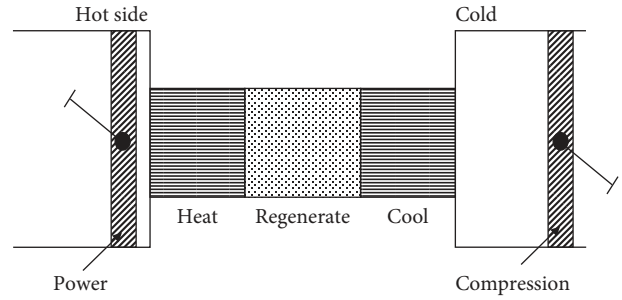

Figure 2: Schematic of alternative design (Stirling cycle), with a regenerator inside the two-piston cylinder.

The heat leak is assumed to occur with constant thermal conductance κ and according to a linear heat transfer law. Viewing κ as a constant is usually a good approximation due to the relatively large heat transfer areas in most cylinders. Hence, the changes in κ that are due to piston motion have a negligible effect. The rate of heat leak Q_{leak} is then given by

$$Q_{\text{leak}} = \kappa\left(T_{\text{wall}} - T_{\text{gas}}\right), \tag{1}$$

where T_{wall} is the temperature of the cylinder wall and T_{gas} is the temperature of the working fluid (ideal gas here), both of which are taken to be spatially uniform.

The rate at which work is dissipated as friction is taken to be comprised of a static term and a dynamic term and is given by

$$\left(\frac{dw}{dt}\right)_{\text{friction}} = \alpha_0\dot{x} + \alpha_1\dot{x}^m, \tag{2}$$

where α_0 and α_1 are constants for the static and dynamic terms, respectively; the exponent m characterizes the dominant type of dynamic friction; and recall that piston velocity $\dot{x}$

is defined as positive. It is important to note that the units of α_1 change with m. For example, $m = 2$ would describe rubbing friction for the piston against a well-lubricated cylindrical surface; and $m = 3$ would pertain to fluid friction when turbulence is induced [25], which might be relevant for modeling losses in engines with internal exchangers, such as Stirling cycles [22–24]. The results will be derived for a general m, and illustrative examples will be presented for $m = 2$ and 3.

In its most general form, the optimization problem can be stated as follows. We aim to maximize the useful work w over a stroke of given, fixed time τ:

$$w = \int_0^\tau \dot{w}\, dt, \tag{3}$$

where we can express $\dot{w} = dw/dt$ as a function f_1 of three variables: piston position x, piston velocity $\dot{x}$, and the internal energy E of the gas and is given by

$$\dot{w} = f_1(x, \dot{x}, E). \tag{4}$$

The expression for $\dot{w}$ will be the difference between the pressure-volume (mechanical $p - V$) work, if any, and the frictional dissipation noted in equation (2) is given by

$$\dot{w} = \delta\left(\frac{R}{C_v}\right)\left(\frac{E\dot{x}}{x}\right) - \alpha_0 - \alpha_1 \dot{x}^m, \tag{5}$$

where $\delta = -1$ for a compression branch, $\delta = 0$ for a constant volume branch, and $\delta = 1$ for an expansion branch.

R is the universal gas constant; C_v is the specific heat at constant volume; and the ideal gas law has been used for the first term on the right-hand-side of equation (5) (for example, in the analyses of [17, 18], $\alpha_0 = 0$ and $m = 2$). It is important to note that, in equations (2)–(5), the absolute value of the velocity is used in the calculations.

A constant volume stroke need not trivially mean a stationary piston. For example, in the Stirling and related cycles, which are double-piston engines for each cylinder, both pistons can move together at the same speed such that no net change occurs in gas volume, yet there are frictional dissipation and heat leak on these strokes (Figure 2). It is for this reason that constant-volume strokes are included in the analysis and refer to strokes where piston motion occurs.

The dynamic constraint for the time evolution of E, as a function f_2 of x, $\dot{x}$, and E, is given by

$$\frac{dE}{dt} = \dot{E} = f_2(x, \dot{x}, E), \tag{6}$$

which in this case is given by

$$\dot{E} = -\delta\left(\frac{R}{C_v}\right)\left(\frac{E\dot{x}}{x}\right) + \beta\left(\alpha_0\dot{x} + \alpha_1\dot{x}^m\right) + \kappa\left(T_{wall} - \frac{E}{nC_v}\right), \tag{7}$$

where β is a dimensionless number between zero and unity that signifies the fraction of heat dissipated as friction that heats up the engine working fluid (for example, in the analyses of [17, 18], $\beta = 0$) and n is the number of gas moles in the cylinder.

We will also need to incorporate a realistic upper bound, a_{max}, on piston acceleration $\ddot{x} \equiv d^2x/dt^2$, which is given by

$$|\ddot{x}| \le a_{max}. \tag{8}$$

The problem can be solved with optimal control theory [26] once the specific modeling assumptions are expressed. We will present solutions for fully externally dissipative friction ($\beta = 0$) and fully internally dissipative friction ($\beta = 1$) (all realistic systems span the intermediate cases).

3. Method of Solution

Following the procedures of optimal control theory [26], we define a modified Lagrangian function L as given by

$$L = \dot{w} - \lambda\left(\dot{E} - f_2(x, \dot{x}, E)\right) = f_1(x, \dot{x}, E) - \lambda\dot{E} + \lambda f_2(x, \dot{x}, E), \tag{9}$$

with all the terms on the right-hand side of equation (9) being given in equations (4)–(7). λ is the Lagrange multiplier and, due to the dynamic constraints, is not a constant but depends on time [26]. The two control variables are taken as x and E, for which the Euler–Lagrange equations are, respectively, given by

$$\left(\frac{\partial L}{\partial x}\right) - \left(\frac{d}{dt}\right)\left(\frac{\partial L}{\partial \dot{x}}\right) = 0, \tag{10a}$$

$$\left(\frac{\partial L}{\partial E}\right) - \left(\frac{d}{dt}\right)\left(\frac{\partial L}{\partial \dot{E}}\right) = 0. \tag{10b}$$

These equations can be arranged in the two coupled equations and are given by

$$\ddot{x} = -\frac{\delta R\beta(1-\lambda)\dot{x}^2}{C_v m(1-\beta\lambda)x} + \frac{\delta R T_{wall}\kappa\left(1-\lambda-\left(E/nC_v T_{wall}\right)\right)}{C_v m(m-1)\dot{x}^{m-2}x(1-\beta\lambda)} + \frac{\beta\kappa\lambda\left(\alpha_0 + \alpha_1 m\dot{x}^{m-1}\right)}{nC_v\alpha_1 m(m-1)\dot{x}^{m-2}(1-\beta\lambda)}, \tag{11a}$$

$$\frac{d\lambda}{dt} = \delta(\lambda - 1)\left(\frac{R}{C_v}\right)\left(\frac{\dot{x}}{x}\right) + \kappa\frac{\lambda}{nC_v}. \tag{11b}$$

Although the initial state of our system is known, the energy at the end of the stroke is not known. Therefore, an additional boundary condition is required [26] and is given by

$$\left(\frac{\partial L}{\partial E}\right)_{t=\tau} = 0, \tag{12}$$

which is equivalent to the following boundary condition as given by

$$\lambda(t = \tau) = 0. \tag{13}$$

In summary, we know the initial conditions

$$\begin{aligned} x(t = 0) &= x_i, \\ E(t = 0) &= E_i, \\ w(t = 0) &= 0, \end{aligned} \tag{14}$$

and the final conditions are given by

$$x(t=\tau)=x_{\mathrm{f}}. \tag{15}$$

Now, we have a set of ordinary differential equations and boundary conditions that can be solved to yield the optimal motion $x(t)$ for producing the power of given stroke, or, equivalently, minimizing dissipated work for a particular stroke. In general, the set of differential equations is not linear and must be solved numerically. However, as will now be argued, realistic engine operating conditions correspond to parameter regimes for which the equations can be solved analytically and in closed form, which makes the solution more transparent and amenable to sensitivity studies.

4. Negligible Role of Heat Leak

For most practical reciprocating engines, on noncombustion strokes, heat leaks are negligible compared to the friction losses and/or $p-V$ work [17, 18, 20–24]. Just as one specific illustrative case, consider a Stirling engine with the compression ratio of 3, $\kappa = 100$ W/K, hydrogen ideal working fluid with $R/C_{\mathrm{v}} = 0.4$, 0.015 kg of gas in the cylinder, a stroke time of 0.008 s, and frictional losses characterized by $m = 2$ in equation (2). It then turns out that the difference in calculated engine power, between the cases of ignoring heat leak and taking it fully into account, is negligible. Even if κ is as much as ten times greater, the error introduced by ignoring it altogether is less than 0.5% (not percentage points). We have confirmed this by generating the exact solution numerically for the above realistic κ value, and then comparing it against the approximate analytic solution, the latter taken at $\kappa = 0$. Therefore, we proceed by generating solutions for the case of $\kappa = 0$; namely, the only dissipation is due to friction. Similar arguments supporting this approximation could be found in [17, 18].

Static friction does not affect the optimal solution; only the dynamic friction term can influence the optimal path. To see this in the governing equations, integrate equations (5) and (7), with negligible heat leak ($\kappa = 0$) to obtain

$$w = E_{\mathrm{i}} - E_{\mathrm{f}} - (1-\beta)\alpha_0 x_{\mathrm{i}}(r-1) - (1-\beta)\alpha_1 \int_0^{\tau} \dot{x}^m\, dt, \tag{16}$$

where E_{f} denotes the energy at the end of the stroke, and

$$\begin{aligned} E_{\mathrm{f}} = {} & E_{\mathrm{i}} r^{-(R/C_{\mathrm{v}})} - \beta \frac{\alpha_0 x_i \left(r - r^{-(R/C_{\mathrm{v}})}\right)}{(R/C_{\mathrm{v}})+1} \\ & - \beta\alpha_1 \left(x_{\mathrm{i}} r\right)^{-(R/C_{\mathrm{v}})} \int_0^{\tau} \dot{x}^m x^{(R/C_{\mathrm{v}})}\, dt, \end{aligned} \tag{17}$$

where r denotes the compression ratio. The path dependence for frictional losses is contained in the dynamic friction terms (α_1 terms) only.

5. Parameters for Conventional Piston Motion

As a basis for later comparison, consider the conventional piston motion, which is approximated here as having a sinusoidal velocity profile (see Figure 3 in the next section):

$$\dot{x}(t) = x_{\mathrm{i}} \frac{(r-1)\pi}{2\tau} \sin\left(\frac{\pi t}{\tau}\right), \tag{18}$$

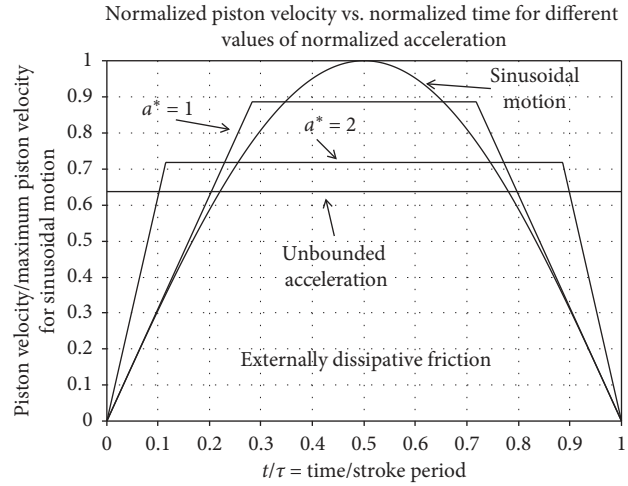

Figure 3: Piston velocity plotted against time, for one engine (expansion) stroke for (1) conventional sinusoidal motion; (2) optimal motion, externally dissipative friction, unbounded acceleration; (3) optimal motion, externally dissipative friction, $a^* = 2$; (4) optimal motion, externally dissipative friction, $a^* = 1$. The abscissa is time divided by stroke time (t/τ), and the ordinate is piston velocity relative to its maximum value for the conventional trajectory. a^* = maximum piston acceleration relative to maximum piston acceleration for sinusoidal motion.

where $x_{\mathrm{i}} = x(t=0)$ is the piston position at the beginning of the stroke and τ is the stroke time. The maximum acceleration for the sinusoidal motion is given by

$$a_{\max}^{\text{sinusoidal}} = x_{\mathrm{i}} \frac{(r-1)\pi^2}{2\tau^2}, \tag{19}$$

which will later serve as a lower bound for the maximum acceleration in the optimal trajectories. In typical reciprocating engines, frictional dissipation results in an efficiency or power loss of 20% [17, 18, 20–24]. Since the optimal trajectories determined below are based on minimizing frictional losses only and should reduce them by 5–75% for realistic engine parameters, and improvements in engine efficiency should be in the range of 1–15%.

6. Solution with Externally Dissipative Friction

Consider the case of externally dissipative friction; namely, $\beta = 0$ in equation (7). This problem was solved in [17] for the case of $m = 2$ (equation (2)), and the optimal solution being that piston velocity should be constant. The solution is unaffected by different values of the exponent m. However, the magnitude of the frictional losses, and the reduction therein relative to conventional piston motion, does depend on the exponent m.

Strictly constant piston velocity, however, would require infinite acceleration at the start of the stroke and infinite deceleration at the end of the stroke. As shown in [17], incorporating the constraint of a given maximum acceleration yields a solution in which the piston is accelerated at its maximum permissible value at the start of

the stroke, followed by constant velocity, and completed by deceleration, at the maximum permissible value and at the end of the stroke (Figure 3) [17]. In the language of optimal control theory, an additional constraint is accounted for (8) with which the Lagrangian is linear in piston acceleration. Hence, piston acceleration has a "bang-bang" solution [26], whereby it assumes its maximum value, and the sign changing (acceleration or deceleration) depends on whether one is at the beginning or at the end of the stroke.

The optimal piston motion for externally dissipative friction is described by the velocity profile [17]:

$$\dot{x} = \begin{cases} a_{\max} t, & 0 \le t \le t_1, \\ a_{\max} t_1, & t_1 \le t \le \tau - t_1, \\ a_{\max} (\tau - t_1), & \tau - t_1 \le t \le \tau, \end{cases} \tag{20}$$

where t_1 is the switching time and is given by

$$t_1 = \frac{\tau}{2} \left(1 - \sqrt{\left(1 - \frac{4 x_i (r-1)}{a_{\max} \tau^2} \right)} \right). \tag{21}$$

7. Reduced Losses with Externally Dissipative Friction

The work dissipated due to friction can now be evaluated for conventional piston motion and optimal piston motion. It is convenient to define nondimensional acceleration, a^*, as the maximum piston acceleration for the optimal path, relative to maximum piston acceleration for sinusoidal motion, and its value is given by

$$a^* = \left(\frac{2\tau^2}{\pi^2 x_i (r-1)} \right) a_{\max}. \tag{22}$$

The optimal switching time t_1 (from the constant acceleration to the constant velocity branch) can then be expressed as

$$t_1 = \frac{\tau}{2} \left(1 - \sqrt{\left(1 - \frac{8}{\pi^2 a^*} \right)} \right). \tag{23}$$

The optimal switching time for this case depends on maximum permissible acceleration only (Figure 4).

As noted above in Section 4, in equations (16) and (17), differences in frictional dissipation due to different piston motions arise solely from dynamic friction, i.e., α_1 term in equation (2). Hence, the problem of evaluating potential improvements in engine efficiency that stem from optimal piston motion reduces to evaluating the reduction in dynamic frictional dissipation only. The ratio of dynamic frictionally dissipated work for conventional piston motion to that for the optimal piston motion can easily be shown as

$$\frac{w_{\text{friction}}^{\text{sinusoidal}}}{w_{\text{friction}}^{\text{optimal}}} = \frac{\pi^{m-1} \Gamma^2 ((m+1)/2)}{\Gamma(m+1) \left(a^* t_1 \pi^2 / 2\tau \right)^m \left(1 - \left(2 m t_1 / (m+1) \tau \right) \right)}, \tag{24}$$

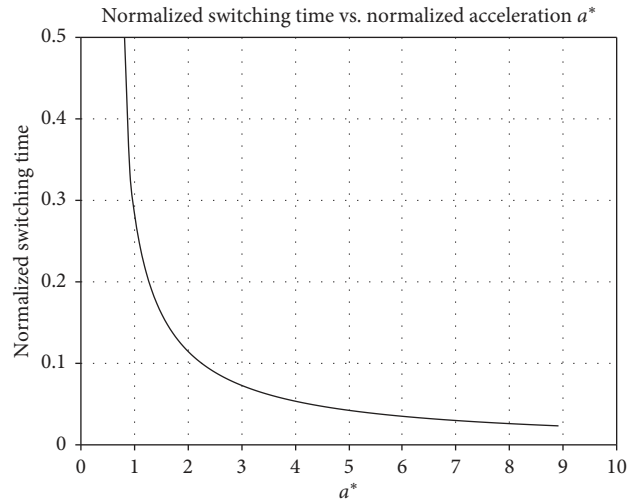

Figure 4: Switching time as a function of a^* in the case of externally dissipative friction.

where Γ denotes the gamma function ($\text{gamma}(\cdot) = \exp(\text{gammaln}(\cdot))$). Note that, with equation (23), the right-hand side of equation (24) depends on a^* only.

Figure 5 shows this relative improvement as a function of nondimensional maximum piston acceleration, for which two values of the frictional exponent m are considered ($m = 2, 3$, equation (2)). In the limit of unbounded acceleration, this improvement is 23% for $m = 2$ and 64% for $m = 3$, with most of these gains already being reached at only twice the maximum acceleration of conventional piston motion. In Figures 3, 5, and 6, our choice of nondimensional variables results in plots that do not have an explicit dependence on the compression ratio.

Figure 6 shows the relative improvement as a function of the frictional exponent (externally dissipative friction) m in the range $2 \le m \le 3$ and for three values of nondimensional maximum piston acceleration: unbounded, 2, and 1.

8. Solution with Internally Dissipative Friction

This case corresponds to solving the governing equations with $\beta = 1$ (and $\kappa = 0$) so that the optimal piston trajectory is described by the following differential equation:

$$\ddot{x} = -\delta \frac{R}{C_v} \frac{1}{m} \frac{\dot{x}^2}{x}. \tag{25}$$

On constant volume strokes, of the type often encountered in Stirling cycles, with $\delta = 0$, the optimal piston trajectory calls for constant velocity. When bounded acceleration is accounted for, the solution of the optimal piston motion is identical to the case with externally dissipative friction, which is analyzed in Section 6.

In the more general case of expansion or compression strokes, the solution to equation (25) for piston velocity is

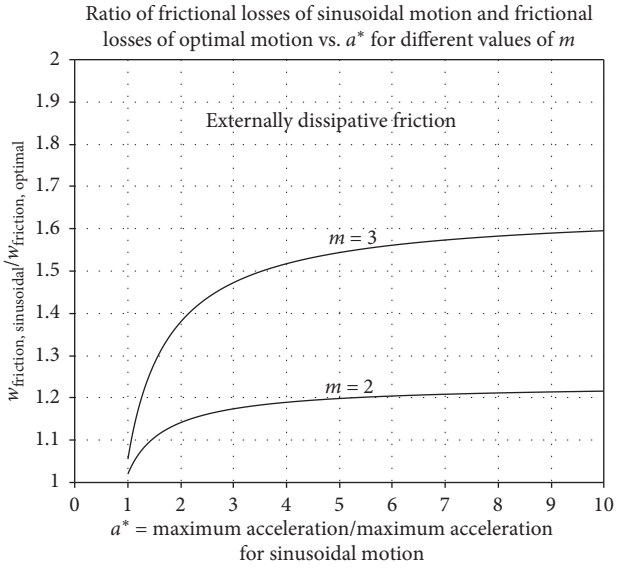

Figure 5: Ratio of work dissipated as friction with conventional piston motion relative to optimal piston motion, plotted against maximum piston acceleration, for two values of frictional exponent m (equation (2)). Maximum piston acceleration is expressed relative to its maximum value for conventional sinusoidal motion.

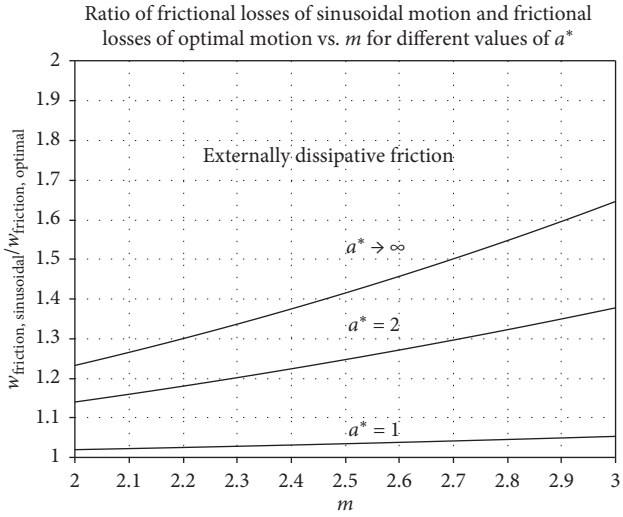

Figure 6: Ratio of work dissipated as friction with conventional piston motion relative to optimal piston motion, plotted against frictional exponent m (equation (2)), for three values of maximum piston acceleration: unbounded acceleration, $a^* = 2$, and $a^* = 1$. Maximum piston acceleration is expressed relative to its maximum value for conventional sinusoidal motion.

$$\dot{x}(t) = \begin{cases} \pi^2 a^* \dfrac{t}{2\tau}, & 0 \le t \le t_1, \\ \pi^2 a^* \dfrac{t}{2\tau}\left(1 + \dfrac{4a^*\pi^2(r-1)t_1(t-t_1)\left((R/mC_v)+1\right)}{2\left(4\tau^2 + a^*\pi^2(r-1)t_1^2\right)}\right)^{-\left((R/mC_v)/\left((R/mC_v)+1\right)\right)}, & t_1 \le t \le t_2, \\ \pi^2 a^* \dfrac{\tau - t}{2\tau}, & t_2 \le t \le \tau, \end{cases} \tag{26}$$

where a^* is the maximum piston acceleration relative to maximum acceleration for conventional trajectory (equation (22)). The optimal switching times for ending the initial constant acceleration branch, t_1, and commencing the final constant deceleration branch, t_2, are not symmetrically located about midstroke, as they were for the case of externally dissipative friction. These optimal switching times are determined by the boundary conditions that (1) piston velocity vanishes at the end of the stroke $(\dot{x}(t = \tau) = 0)$ and (2) the final position is known $(x(t = \tau) = x_f)$. They can be obtained numerically as the solutions to the following two coupled nonlinear equations:

$$\begin{aligned} t_2 &= \tau \\ &\quad - t_1\left(1 + \frac{4a^*\pi^2(r-1)t_1(t_2-t_1)\left((R/mC_v)+1\right)}{2\left(4\tau^2 + a^*\pi^2(r-1)t_1^2\right)}\right)^{-\left((R/mC_v)/\left((R/mC_v)+1\right)\right)}, \\ r &= \frac{a^*\pi^2(r-1)(\tau - t_2)^2}{4\tau^2} + \left(1 + \frac{a^*\pi^2(r-1)t_1^2}{4\tau^2}\right) \\ &\quad \cdot \left(1 + \frac{4a^*\pi^2(r-1)t_1(t_2-t_1)\left((R/mC_v)+1\right)}{2\left(4\tau^2 + a^*\pi^2(r-1)t_1^2\right)}\right)^{-\left((R/mC_v)/\left((R/mC_v)+1\right)\right)}. \end{aligned} \tag{27}$$

Illustrations of optimal motion and conventional piston motion, when friction is dissipated internally, are presented in Figures 7 and 8. These include sensitivity study to key system parameters, such as compression ratio, maximum piston acceleration, and frictional exponent in equation (2).

9. Reduced Losses with Internally Dissipative Friction

Recall that to determine the potential improvement due to optimal piston motion, one needs to evaluate only the reduction in dynamic frictional dissipation. Dynamic frictional dissipation for the conventional and the optimal trajectories can be evaluated via numerical integration or analytically with the evaluation of hypergeometric functions.

Graphical illustrations of the magnitude of this improvement and how it depends on key system parameters are presented in Figures 9 and 10. Although the shapes of the ordinates approximately appear constant, their numerical values change between 1.2 and 1.3 for $m = 2$ and between 1.65 and 1.75 for $m = 3$. The changes are nonlinear in behavior.

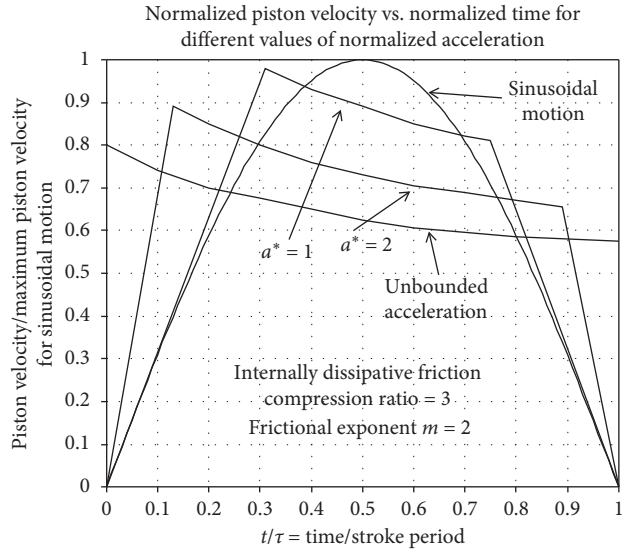

Figure 7: Piston velocity plotted against time, for one engine (expansion) stroke for (1) conventional sinusoidal motion; (2) optimal motion, internally dissipative friction, unbounded acceleration; (3) optimal motion, internally dissipative friction, $a^* = 2$; (4) optimal motion, internally dissipative friction, $a^* = 1$. The abscissa is time divided by stroke time (t/τ), and the ordinate is piston velocity relative to its maximum value for the conventional trajectory.

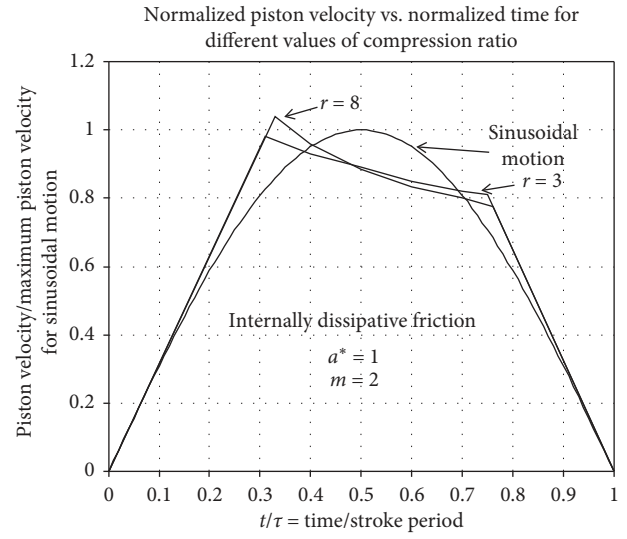

Figure 8: Example of sensitivity of optimal piston motion to compression ratio r, for internally dissipative friction. Maximum nondimensional piston parameter $a^* = 1$. Frictional exponent $m = 2$. Plots are for (1) conventional motion; (2) optimal motion with $r = 3$; (3) optimal motion with $r = 8$. The abscissa is time divided by stroke time (t/τ), and the ordinate is piston velocity relative to its maximum value for the conventional trajectory.

The potential improvement in engine efficiency is slightly larger than that for the externally dissipative case. The influence of compression ratio is modest, whereas the functional form of frictional losses, and piston maximum acceleration, can have a marked effect on the relative improvement in engine power.

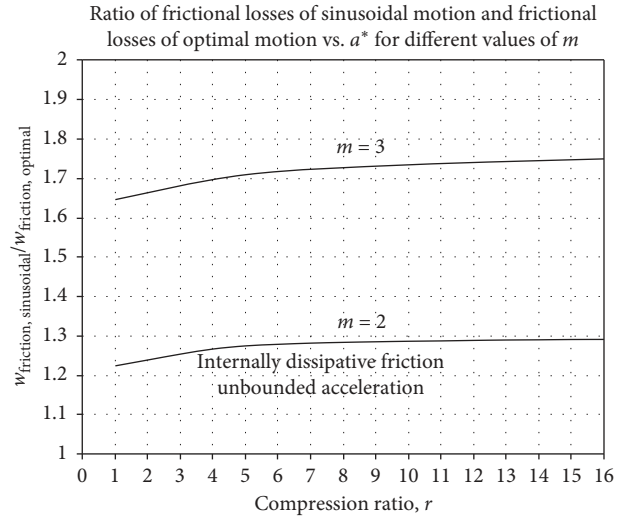

Figure 9: Sensitivity to compression ratio of reduction in frictional losses. Calculations are for unbounded acceleration. Ordinate is dynamic frictional losses for conventional piston motion relative to that for optimal piston motion, for internally dissipative friction. Abscissa is the compression ratio. The two curves are for different frictional exponents m and show the marked dependence on m.

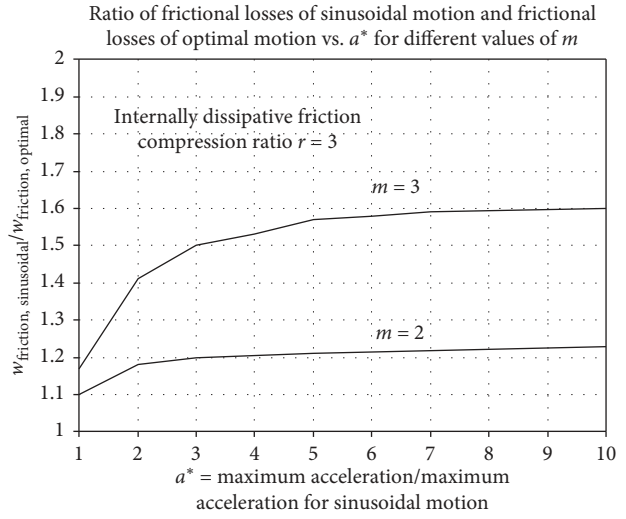

Figure 10: Sensitivity of reduction in frictional losses to maximum piston acceleration. Ordinate is dynamic frictional losses for conventional piston motion relative to that for optimal piston motion, for internally dissipative friction. Abscissa is maximum piston acceleration relative to its maximum value for the conventional trajectory. The two curves are for different frictional exponents m and show the marked dependence on m.

10. Summary and Conclusions

One prospective method to increase the efficiency and power of reciprocating engines is to reduce frictional losses by modifying piston motion. The purpose of this paper (study) is to determine piston trajectories that are optimal for noncombustion strokes in reciprocating engines, in the sense of minimizing frictional dissipation and hence

maximizing efficiency and power. The potential improvements in overall engine efficiency have also been evaluated and should lie in the range of around 2–10%, depending on how severe frictional losses were prior to the modification of piston motion. The optimized engine strokes that we have calculated could serve as building blocks in the construction of optimal cycles in external combustion of optimal cycles in the external combustion engines and for noncombustion strokes in internal combustion engines.

Several qualifications are in order. First, no experimental verification has yet been attempted. Second, specific functional forms for frictional losses have been assumed. However, these forms appear to cover the behavior of real engines [20–24], with friction stemming from static, surface rubbing friction, and fluid turbulence contributions. Third, altering piston motion engenders changes in standard crankshafts, which in turn can change frictional losses external to the engine. These could improve or worsen overall engine efficiency, depending on how such crankshafts would be designed and built. This issue is not analyzed here.

Optimal piston motion turns out to be sensitive to where the heat generated by frictionally dissipated work goes: either to an external cooling system (externally dissipative), or to heating the engine working fluid (internally dissipative), or, in reality, somewhere between these two extremes. We have derived closed-form analytic solutions for optimal piston motion for both cases and compared them to conventional sinusoidal piston paths.

The improvement in engine efficiency for the optimal paths, relative to conventional piston motion, turns out to be mildly sensitive to compression ratio, with a significant effect arising from the functional form of frictional losses and from maximum piston acceleration. Only when piston accelerations in excess of those achievable with conventional sinusoidal motion can be reached will the improvements in engine efficiency be substantial. Fortunately, these improvements in engine efficiency increase rapidly with maximum attainable acceleration for values just above those of conventional motion and then asymptote (Figures 5 and 10).

The mechanisms to achieve the optimal piston motion and the experimental verification of the optimal piston motion are two good research ideas for future research.

Data Availability

The data used to support the findings of this study are included within the article.

Conflicts of Interest

The author declares that he has no conflicts of interest.

References

[1] C. F. Taylor, *The Internal-Combustion Engine in Theory and Practice*, MIT Press, Cambridge, MA, USA, 1971.

[2] A. M. K. P. Taylor, "Science review of internal combustion engines," *Energy Policy*, vol. 36, no. 12, pp. 4657–4667, 2008.

[3] F. L. Curzon and B. Ahlborn, "Efficiency of a carnot engine at maximum power output," *American Journal of Physics*, vol. 43, no. 1, pp. 22–24, 1975.

[4] B. Andresen, "Current trends in finite-time thermodynamics," *Angewandte Chemie*, vol. 50, no. 12, pp. 2690–2704, 2011.

[5] R. Mikalsen, Y. D. Wang, and A. P. Roskilly, "A comparison of Miller and Otto natural gas engines for small scale CHP applications," *Applied Energy*, vol. 86, no. 6, pp. 922–927, 2009.

[6] F. Angulo-Brown, J. Fernández-Betanzos, and C. A. Diaz-Pico, "Compression ratio of an optimized air standard Otto-cycle model," *European Journal of Physics*, vol. 15, no. 1, pp. 38–42, 1994.

[7] J. M. Gordon and M. Huleihil, "General performance characteristics of real heat engines," *Journal of Applied Physics*, vol. 72, no. 3, pp. 829–837, 1992.

[8] J. M. Gordon, "Generalized power versus efficiency characteristics of heat engines: the thermoelectric generator as an instructive illustration," *American Journal of Physics*, vol. 59, no. 6, pp. 551–555, 1991.

[9] Y. Zhaoa and J. Chen, "Performance analysis of an irreversible Miller heat engineand its optimum criteria," *Applied Thermal Engineering*, vol. 27, no. 11-12, pp. 2051–2058, 2007.

[10] Y. Ge, L. Chen, F. Sun, and C. Wu, "Performance of an Atkinson cycle with heat transfer, friction and variable specific heats of working fluid," *Applied Energy*, vol. 83, no. 11, pp. 1210–1221, 2006.

[11] A. C. Hernandez, A. Medina, J. M. M. Roco, and S. Velasco, "On an irreversible air standard Otto-cycle model," *European Journal of Physics*, vol. 16, no. 2, pp. 73–75, 1995.

[12] F. Angulo-Brown, J. A. Rocha-Martínezand, and T. D. Navarrete-González, "A non-endoreversible Otto cycle model: improving power output and efficiency," *Journal of Physics D: Applied Physics*, vol. 29, no. 1, pp. 80–83, 1996.

[13] P. S. Kuo, "Cylinder pressure in spark-ignition engine: a computational model," *Journal of Undergraduate Sciences*, vol. 3, pp. 141–145, 1996.

[14] R. Masoudi Nejad, "Power output and Efficiency of internal combustion engine based on the FTT theory," *Life Science Journal*, vol. 9, no. 1, 2012.

[15] M. Huleihil, "Effects of pressure drops on the performance characteristics of air standard Otto cycle," *Physics Research International*, vol. 2011, Article ID 496057, 7 pages, 2011.

[16] H. S. Leff, "Thermal efficiency at maximum work output: new results for old heat engines," *American Journal of Physics*, vol. 55, no. 7, pp. 602–610, 1987.

[17] M. Mozurkewich and R. S. Berry, "Optimal paths for thermodynamic systems: the ideal Otto cycle," *Journal of Applied Physics*, vol. 53, no. 1, pp. 34–42, 1982.

[18] K. H. Hoffman, S. J. Watowich, and R. S. Berry, "Optimal paths for thermodynamic systems: the ideal Dusel cycle," *Journal of Applied Physics*, vol. 58, no. 6, pp. 2125–2134, 1985.

[19] L. Chen, Sh. Xia, and F. Sun, "Optimizing piston velocity profile for maximum work output from a generalized radiative law Diesel engine," *Mathematical and Computer Modelling*, vol. 54, no. 9-10, pp. 2051–2063, 2011.

[20] J. B. Heywood, *Internal Combustion Engine Fundamentals*, McGraw-Hill, New York, NY, USA, 1988.

[21] C. F. Taylor, *The Internal Combustion Engine in Theory and Practice*, MIT press, Cambridge, MA, USA, 1968.

[22] G. T. Reader and C. Hooper, *Stirling Engines*, E. & F.N. Spon, London, UK, 1983.

[23] I. Urieli and D. M. Berchowich, *Stirling Cycle Engine Analysis*, A. Hilger, Bristol, UK, 1984.

[24] C. M. Hargreaves, *The Philips Stirling Engine*, Elsevier, Amsterdam, Netherlands, 1991.
[25] L. D. Landu and E. M. Lifshitz, *Fluid Mechanics, Second English Edition*, Vol. 6, Pergamon Press, New York, NY, USA, 1987.
[26] D. Burghes and A. Graham, *Introduction to Control Theory Including Optimal Control*, Wiley, New York, NY, USA, 1980.